Regular/irregular phase space structure of HCN/HNC

M. Founargiotakis, S. C. Farantos, and J. Tennyson

Citation: J. Chem. Phys. **88**, 1598 (1988); doi: 10.1063/1.454138
View online: http://dx.doi.org/10.1063/1.454138
View Table of Contents: http://jcp.aip.org/resource/1/JCPSA6/v88/i3
Published by the American Institute of Physics.

Regular/irregular phase space structure of HCN/HNC

M. Founargiotakis and S. C. Farantos
Department of Chemistry, University of Crete and Institute of Electronic Structure and Lasers, Research Center of Crete, Iraklion, 711 10 Crete, Greece

J. Tennyson
Department of Physics and Astronomy, University College London, Gower Street, London WC1E 6BT, England

(Received 20 April 1987; accepted 29 September 1987)

A detailed 3D classical nonlinear mechanical analysis of HCN/HNC system is carried out and the results are compared with 2D quantum mechanical vibrational calculations as well as with the recent 3D quantum calculations of Bacic and Light. HCN is marked by regular behavior which persists at high energies when the stretching modes are excited. Chaotic trajectories located in the HNC well are those which lead to isomerization of HNC. The regular/irregular phase space structure agrees well with the corresponding assignment of quantum states. A multiple resonance among the vibrational modes of HCN, located at the top of the effective barrier of isomerization, is considered as the classical cause of the lack of delocalization of the wave functions found in the 3D quantum calculations.

I. INTRODUCTION

The advance of nonlinear mechanics has had a great influence on molecular dynamics both theoretically[1] and experimentally.[2] The transition from regular to irregular motion, common to most nonlinear dynamical systems,[3] is expected to have a counterpart in molecules. One should be able to recognize chaotic states in spectroscopy and chemical dynamics although molecules are governed by quantum mechanics. Although there is no indisputable definition of "quantum chaos" there is much evidence that molecular wave functions and eigenvalues have different properties at energies where regular or chaotic classical motion predominates.[1] Regions of phase space where the trajectories are quasiperiodic and localized also correspond to mode localized wave functions which show a remarkable regularity in their nodal structure. In contrast wave functions with irregular nodal patterns are often delocalized and they are found at energies where classical trajectories are highly chaotic.[4–10] The nearest neighbor level spacing distribution has also been proposed as a criterion of quantum chaos giving Poisson (exponential) type distributions[11] for regular states and Wigner type for irregular states.[12] The drawbacks of the above criteria for quantum chaos have been discussed in the literature.[1,5]

Chaos appears in multidimensional systems; for generic Hamiltonians, quasiperiodic and chaotic trajectories coexist at the same total energy.[3] For molecules it is expected that the transition from regular to irregular motion will depend on the method of excitation. Thus questions such as (i) does rotational excitations lead to chaotic behavior or (ii) which vibrational mode should be excited in order to achieve localized states in highly excited molecules, are important. Answers to these questions are vital for understanding spectroscopy and chemical dynamics.

In a recent series of papers[5–9] we have examined the classical and quantum vibrational motion of the floppy molecules KCN, LiCN, and ArHCl. The main conclusions are: (i) quantum mechanical behavior mimics the classical. That means that regular/irregular or mode localized/delocalized states are found in both mechanics but the onset of quantum chaos occurs at higher energies than in classical dynamics. (ii) There is a specificity in the appearance of chaos in overtone excitations. The excitation of the bending mode leads to irregular behavior at lower energies than excitation of the stretching modes for LiCN. (iii) The vibrational spectra of LiCN are sharp with large intensities for regular states and broad of low intensity for the chaotic states in agreement with Percival's conjecture stated years ago.[13] Similar behavior has recently been predicted for RbCN.[14] (iv) KCN shows are early, strong mode mixing and chaotic trajectories exist even at the zero point energy (zpe). These studies suggest that by replacing a heavy atom (K) with a lighter atom (Li), the measure of regular component of phase space increases. Therefore, in order to test this trend it is natural to extend our studies to a third member of this family of compounds, HCN. In this article we report a detailed study of the phase space structure of HCN/HNC together with quantum mechanical calculations of the vibrational levels and for J, the quantum number of the total angular momentum, equal to zero. The role of rotational excitation in the onset of chaos has only recently attracted some interest.[15,16] However since the available quantum mechanical calculations[17] are for a rotationless molecule we study only vibrational excitation.

There have been several calculations on the vibrational levels of HCN and the isomerization process HNC→HCN. An *ab initio* potential energy surface and vibrational adiabatic type calculations have been performed by Peric *et al.*[18] in a theoretical investigation of HNC→HCN isomerization. Bacic, Gerber, and Ratner[19] have used optimal coordinates in a self-consistent-field method to evaluate the vibrational levels and the tunneling dynamics of HCN. In this study the authors used the potential function of Murrell, Carter, and Halonen[20] which is valid in the full nuclear configuration space. A modified version of this potential function was pro-

 0021-9606/88/031598-10$02.10

duced by Holme and Hutchinson[21] and used in a classical mechanical study of HNC→HCN isomerization. It was found that the isomerization rate is enhanced nonstatistically by a resonance energy transfer which involves overtone excitation of the HX stretching mode and coupling with the CN and bending modes.

In a very recent article Bacic and Light[17] calculated highly excited vibrational energies of HCN/HNC for the three modes of the molecule using the potential energy surface of Murrell *et al.*[20] One hundred and ten levels were calculated and about 65 of them lie above the barrier to isomerization. The authors examine the localization of the wave functions in the HCN well by computing the relative amplitudes on each side of the isomerization barrier. In addition they find that the nearest neighbor level spacing distribution is Poisson type thus indicating the regular behavior of the molecule up to the energy studied. Spectroscopic studies support the theoretical results. Lehmann, Scherer, and Klemperer[22] obtained simple, regular vibrational spectra for the stretching modes of HCN. The investigators attempted a parallel classical trajectory study in order to identify experimentally features of chaos.

All these articles demonstrate that HCN provides a prototype system for studying intramolecular dynamics in triatomic species. The realistic potential function of Murrell *et al.*,[20] although it is not expected to be accurate at high energies, reproduces the basic topographical characteristics of the surface. Thus a detailed 3D classical trajectory analysis of HCN/HNC at a range of energies up to the dissociation limit seems appropriate. In this article we make a comparison of the classical picture with the 3D quantum calculations of Bacic and Light.[17] We have also carried out 2D quantum mechanical calculations by freezing the CN bond at its equilibrium point and the results are compared with the 3D ones. The 2D computations allow us to plot the wave functions and recognize their nodal structure for a larger number of energy levels above the barrier than the 3D calculations.

II. COMPUTATIONAL METHODS

The Murrell, Carter, Halonen[20] potential function is employed in the present calculations. The main topographical characteristics are the two minima corresponding to the HCN (absolute minimum) and HNC (relative) with an energy difference of 3883 cm^{-1} and a potential barrier of 12 150 cm^{-1} relative to the HCN. The lowest dissociation channel, removal of the hydrogen atom, is 45 676 cm^{-1} above the absolute minimum. Comparing the minimum energy path for isomerization of the empirical function with the *ab initio* one of Peric *et al.*[18] showed a plateau in the former potential in the HNC well at about 3100 cm^{-1} above the HNC minimum. This is an artifact of the empirical function and we shall see that this feature influence the classical dynamics. Holme and Hutchinson[21] found a minimum in the exit channel of the dissociating hydrogen atom. These artifacts of the potential do not invalidate the general conclusions which we draw from the classical and quantum calculations, but they would be crucial for a quantitative comparisons with the experimental results.[22]

In the previous publications we have described the methods used in distinguishing regular/chaotic trajectories and quantum states.[5–10] Here we give a few details related to the calculations of the rotationless HCN. Trajectories were integrated using valence coordinates; the bond lengths R_{HC}, R_{CN}, and the angle between them φ. Initial conditions were chosen by using the three normal coordinates. The regular/chaotic nature of the trajectories is found by plotting Poincaré surfaces of section,[1] power spectra of the dynamical variables[1] and calculating the six Lyapunov exponents[23–25] λ_i, $i = 1, \ldots, 6$. It is has been proved that for Hamiltonian systems

$$\lambda_\varkappa = -\lambda_{7-\varkappa}, \quad \varkappa = 1,2,3. \tag{1}$$

Because of the conservation of total energy, two exponents are zero. Generally the number of zero Lyapunov exponents is associated with the number of constants of motion.[25] For a system with three degrees of freedom there are three possibilities: (i) all Lyapunov exponents are zero and the trajectories are quasiperiodic, (ii) there are two positive Lyapunov exponents for the chaotic trajectories, and (iii) there is only one positive Lyapunov exponent. In the latter case, chaos is restricted to a subspace of the energy shell. Although there is numerical evidence to support this intermediate case,[26] Arnold diffusion[3] guarantees that the chaotic regions of phase space are interconnected in contrast to 2D systems where chaotic regions may be isolated between regular regions. However Nekhoroshev's theorem[27] states that Arnold diffusion in some action variables may take a very long time and thus a chaotic trajectory remains in a subspace of the phase space. In this case it is acceptable to talk about approximately conserved quantities.[28] For the computation of Lyapunov exponents we use the numerical algorithm of Wolf *et al.*[23]

Visualization of the trajectories is achieved by taking cuts of the trajectories with one plane defined at the equilibrium value of one of the valence coordinates and the corresponding momentum greater than zero. Thus for a particular plane (say $R_{HC} = 2.0135\, a_0$) we produce two surfaces of section (R_{CN}, P_{CN}) and (φ,P_φ). Similarly for the planes $R_{CN} = 2.1792\, a_0$ and $\varphi = \pi$ we produce another four surfaces of section which allow a detailed inspection of the trajectory. For 3D systems, the tori are three dimensional and the cuts with a plane form two-dimensional surfaces. Cuts of the trajectories with two planes simultaneously (say R_{HC} and R_{CN}) could produce 1D surfaces of section but this requires very long times of integration. Even so they have been used by Noid *et al.*[29] for a semiclassical quantization of some 3D potentials. However, as is shown later in our case of a multiple resonance among the three oscillators, the one-plane cuts also produce smooth curves around a stable periodic orbit. From the number of islands on each plane we can assign the resonance. To calculate surfaces of section we have used the technique proposed by Henon[30] which is quite efficient for the present three dimensional system.

The quantum calculations were performed in generalized scattering coordinates.[31] These were defined as R, the distance of H from a point X on the CN bond and the angle θ give by $H\hat{X}N$. The CN bond length r was kept constant at 2.179 a_0. IF X is chosen as the center of CN mass, then one obtains the usual scattering coordinates. Preliminary calcu-

TABLE I. 2D vibrational levels of HCN/HNC relative to the ground state. Levels with the character U means that the assignment is uncertain, D means delocalized. The quantum numbers in brackets denote the vibrational levels of HNC. E_{3D} are the 3D results of Bacic and Light (Ref. 17).

N	$n_1n_2n_3$	Ch	E_{2D}	E_{3D}	ΔE
1	0 0 0			3 483	
2	0 2 0		1 430	1 418	− 12
3	0 4 0		2 831	2 806	− 25
4	0 0 1		3 197	3 318	+ 121
5	[0 0 0]		3 921	3 808	− 113
6	0 6 0		4 199	4 161	− 38
7	0 2 1		4 608	4 707	+ 99
8	[0 2 0]		4 881	4 751	− 130
9	0 8 0		5 528	5 477	− 51
10	[0 4 0]		5 760	5 625	− 135
11	0 4 1		5 989		
12	0 0 2		6 285	6 531	+ 246
13	[0 6 0]		6 431	6 327	− 104
14	[0 8 0]		6 750	6 649	− 111
15	0 10 0		6 812		
16	[0 10 0]		7 194	7 048	− 146
17	0 6 1		7 335		
18	[0 0 1]		7 465	7 440	− 25
19	0 2 2		7 677		
20	[0 12 0]		7 710	7 538	− 172
21	0 12 0		8 043		
22	[0 14 0]		8 287	8 094	− 193
23	[0 2 1]		8 401	8 351	− 50
24	0 8 1		8 641		
25	[0 16 0]		8 908		
26	0 4 2		9 038		
27	0 14 0		9 209		
28	[0 4 1]		9 264		
29	0 0 3		9 270		
30	[0 18 0]		9 561		
31	[0 6 1]		9 882		
32	0 10 1		9 901		
33	[0 8 1]	U	10 084		
34	[0 20 0]		10 227		
35	0 16 0		10 283		
36	0 6 2		10 362		
37	[0 10 1]	U	10 532		
38	0 2 3		10 644		
39	[0 22 0]		10 866		
40	[0 0 2]		10 869		
41	[0 12 1]	U	11 022		
42	0 12 1		11 106		
43	0 18 0	U	11 202		
44	0 22 0	D	11 492		
45	[0 14 1]	U	11 571		
46	0 8 2		11 646		
47	[0 1 2]	D	11 782		
48	0 23 0	D	11 932		
49	0 4 3		11 985		
50	[0 16 1]	U	12 152		
51	0 0 4		12 169		
52	0 14 1		12 243		
53	0 24 0	D	12 311		
54	[0 4 2]		12 631		
55	0 25 0	U	12 734		
56			12 815		
57	0 10 2		12 883		
58	[0 6 2]	U	13 110		
59	0 26 0	D	13 213		
60	0 6 3	U	13 280		
61	0 16 1	U	13 291		
62	[0 8 2]	U	13 333		
63			13 432		
64	0 2 4		13 523		
65	0 0 2		13 729		
66	[0 10 2]	U	13 756		
67			13 977		
68	0 12 2	U	14 062		
69	[0 0 3]		14 131		
70			14 170		
71			14 224		
72	0 28 0	U	14 287		
73	0 8 3		14 552		
74	0 22 1	U	14 564		
75			14 717		
76	0 29 0		14 810		
77	0 4 4		14 846		
78	0 23 1	U	14 985		
79	[0 2 3]		15 020		
80	0 0 5		15 065		

lations[32] showed that a better choice, for variational convergence of the vibrational states, was to define X such that the distance HX was equal for the two linear minima on the surface. This cooresponds to a value of $g^{31} = XN/CN = 0.531$. Results were obtained using program TRIATOM[33] and a basis set which consisted of 14 Morse-oscillator-like functions (with $R_e = 2.705\ a_0$, $D_e = 3.0\ E_h$, and $\omega_e = 0.0096\ E_h$) and 51 Legendre functions.

Eighty vibrational levels were computed covering an energy region up to 18 500 cm^{-1} (energies are measured from the minimum of the potential except if it is stated otherwise) the highest of these are converged to within 10 cm^{-1}. Quantum 3D calculations have performed by Bacic and Light[17] for 110 vibrational levels and energies up to 15 254 cm^{-1}. Our full 3D quantum mechanical calculations agreed well with Bacic and Light, showing that there is a discrepancy in the published vibrational band origins of Murrell *et al.*[20] (see footnote 14 of Ref. 17). However, we were unable to get satisfactory convergence for states in the region of the barrier in the 3D calculations. Therefore we use their results for comparison with the 3D classical calculations. A comparison of 2D to 3D results of Bacic and Light[17] is shown in Table I for those levels which have been assigned quantum numbers. The energies are measured relative to the zpe. Of course the assignment in Table I which were obtained by inspection of the nodal pattern of the wave functions, all correspond to $n_1 = 0$ for the quantum number of the CN stretch. We observe that in the 2D calculations the bending overtones are overestimated but the stretching fundamental (n_3) and overtone are underestimated.

III. RESULTS

A. Quantum picture

The 2D wave functions for all computed levels have been plotted and from the nodal patterns the states have been assigned quantum numbers for either HCN or HNC. Those states which are delocalized are labeled with the letter D. We distinguish the following types of states; (i) localized HCN (Fig. 1), (ii) localized HNC (Fig. 2), (iii) rotating regular states (polytopic) (Fig. 3), and (iv) delocalized irregular states (Fig. 4). Below the barrier to isomerization the states are regular and localized in both 2D and 3D calculations. In

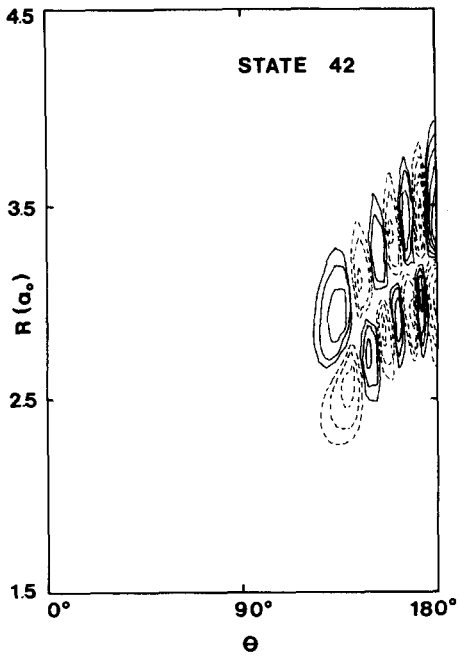

FIG. 1. Nodal structure of a typical regular/localized state (0 6 1) of HCN. The contours link points where the wave function has 4%, 8%, 16%, 32%, and 64% of the maximum amplitude. Solid (dashed) curves are for positive (negative) amplitude.

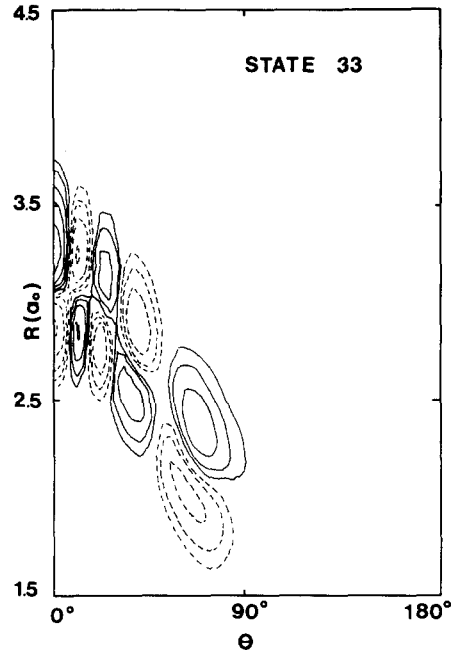

FIG. 2. A typical regular/localized HNC state, contours as in Fig. 1.

Bacic and Light's 3D calculations, most of these states were assigned quantum numbers from the predominant coefficient in the expansion of the eigenfunctions. The localization of the wave functions is preserved even above the isomerization barrier: up to 14 685 cm^{-1} which is the 43rd state in Table I. The next state is clearly a rotating type and can be assigned as (0 22 0); it is shown in Fig. 3(a). In the 3D calculations, the first significantly delocalized state is at 14 582 cm^{-1}, with a relative amplitude of the wave function in the HCN well equal to 0.86. Above this, another 17 states were computed by Bacic and Light, up to the energy 15 254 cm^{-1}, but none of them shows large delocalization.

In the 2D results, we find that above the 44th state there is a significant number of polytopic states [Fig. 3(b)] and only states with three or more quanta in the stretching mode remain localized in the HCN or HNC wells. Even a rotating type state with one quantum in the stretching mode has been identified (Fig. 5). All the states above the 47th in Table I have energies larger than the highest 3D state calculated. However, the bending overtones are overestimated in the 2D

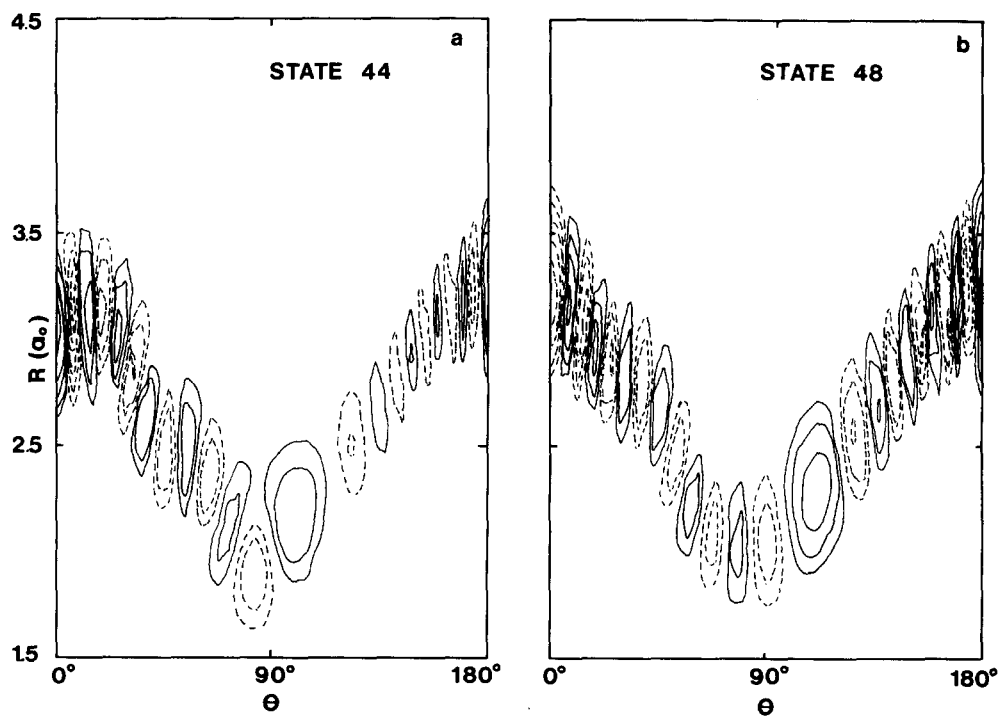

FIG. 3. Typical rotating (polytopic) states, contours as in Fig. 1.

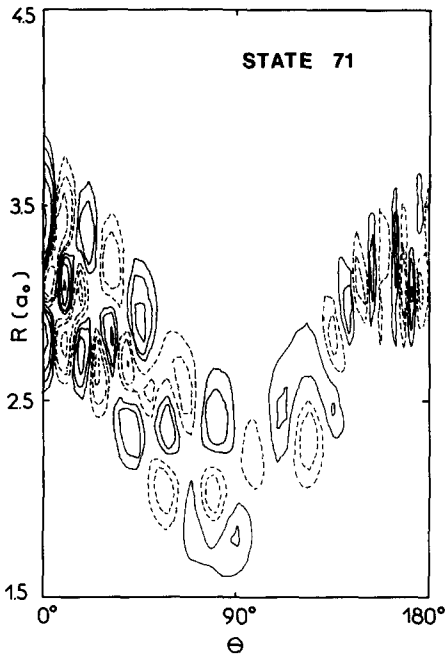

FIG. 4. A typical irregular/delocalized state, contours as in Fig. 1.

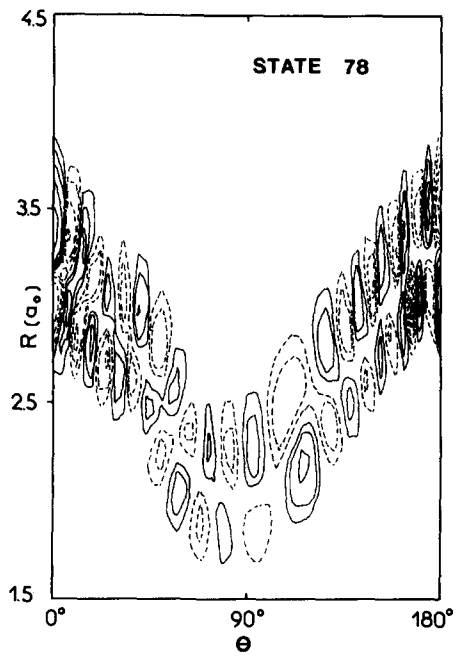

FIG. 5. A rotating-type state with the stretching mode excited, contours as in Fig. 1.

computations and therefore should correspond to lower states in the 3D calculations.

To summarize, the 2D and 3D quantum mechanical calculations show that regular localized states exist up to about 2400 cm^{-1} above the potential barrier of isomerization. Above this energy a significant number of the 2D states are delocalized and are associated either with regular polytopic states or irregular ones. However, the degree of nodal struc-

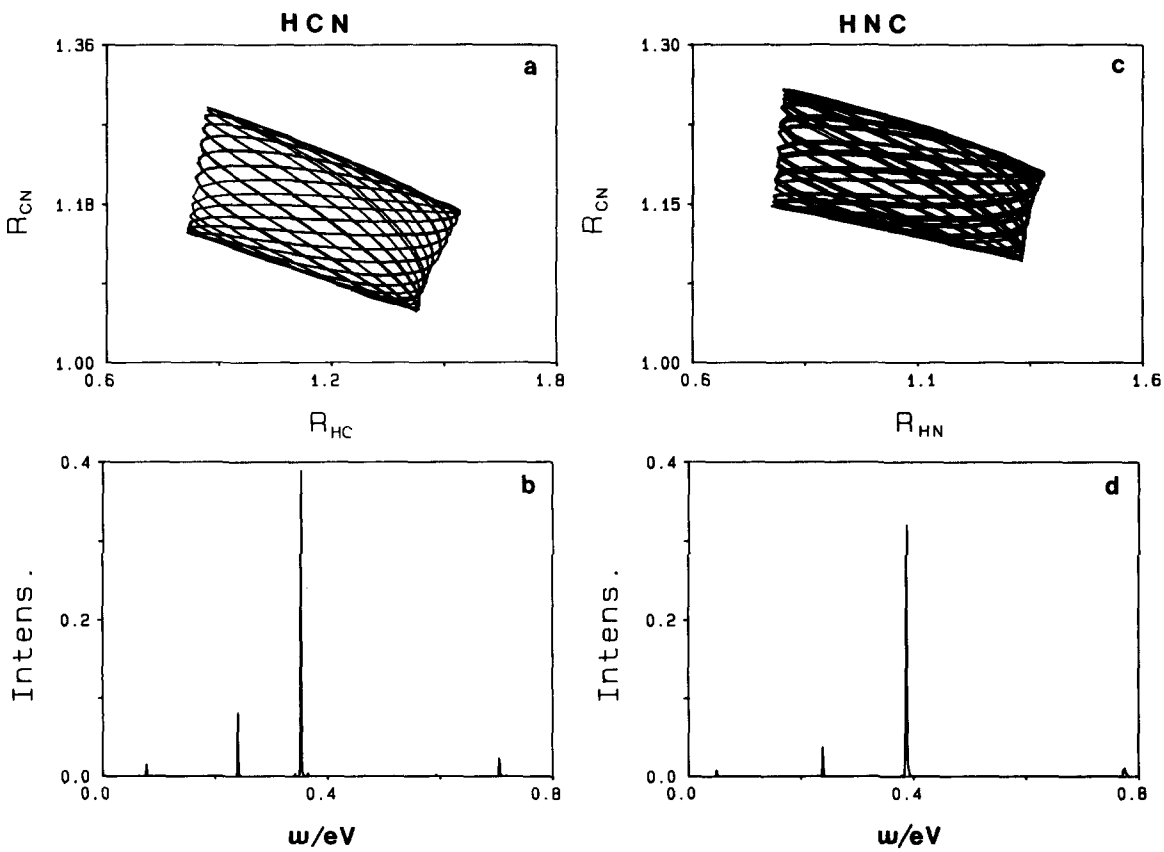

FIG. 6. Quasiperiodic trajectories localized in HCN (a), (b) and HNC (c), (d) minima. Shown are the projections of two trajectories in R_{HC}/R_{HN} and R_{CN} coordinate plane and the power spectra of the sum of the three conjugate momenta. Both trajectories are for energies above the barrier; $E = 17\,026\ cm^{-1}$ and $E = 18\,486\ cm^{-1}$.

ture complexity is not so large as that fond in LiCN. HCN/HNC are generally regularly behaved species.

B. Classical picture

The classical trajectories studied were initialized by using a zero-order harmonic approximation with equilibrium points either in the HCN or HNC minimum. We distinguish the following types of trajectories; (i) regular localized in the HCN well below and above the barrier (Fig. 6), (ii) regular trajectories localized in the HNC well below and above the barrier (Fig. 6), (iii) delocalized chaotic trajectories (Fig. 7), and (iv) chaotic localized trajectories in the HNC well (Fig. 7).

By studying trajectories obtained with overtone excitations of the three normal modes of HCN we draw the following phase space structure. Quasiperiodic trajectories are found up to about 40 000 and 28 000 cm^{-1} by exciting the CH- and CN- normal modes, respectively. It is worth mentioning that the onset of extended stochasticity by exciting the CH mode is only 5700 cm^{-1} below the first dissociation channel and about 27 000 cm^{-1} above the potential barrier to isomerization. In contrast by exciting the bending mode of HCN chaotic trajectories emerge just above the effective barrier (the potential barrier plus the zpe of the two stretching modes). In fact, it is these trajectories which can escape to the HNC well. Examination of the trajectories initialized by exciting the normal modes of HNC indeed reveal that chaotic trajectories can be obtained 3000 cm^{-1} above the HNC minimum by exciting the bending mode. This is where the plateau on the reaction path appears.

Surprisingly it is found that trajectories which have enough energy in the bending mode of HCN and zpe in the stretching modes can be trapped in the HCN minimum and do not isomerize. In Fig. 8, the number of trapped trajectories integrated for 8 ps is shown as a function of the energy above the barrier. The lifetime distribution at 1058 cm^{-1} is also shown.

What causes the trapping? We have examined the trapped trajectories by plotting the surfaces of section on each of the planes R_{HC}, R_{CN}, and φ. Five typical trajectories are shown in Fig. 9. We can see that a number of stability islands appear on each plane. For instance for fixed R_{HC} there are three islands on the (R_{CN}, P_{CN}) plane and six on the (φ, P_φ) plane. For fixed R_{CN}, there are two and four islands on the (R_{HC}, P_{HC}) and (φ, P_φ) planes, respectively. For fixed φ, only one island appears on the (R_{HC}, P_{HC}) and (R_{CN}, P_{CN}) planes (not shown). From the power spectra of the trajectories inside the islands, the ratio of pairs of frequencies is found to be

$$\frac{\omega_{HC}}{\omega_\varphi} \approx \frac{6}{1} \quad \text{and} \quad \frac{\omega_{CN}}{\omega_\varphi} \approx \frac{4}{1}. \tag{2}$$

These two equations also imply that $\omega_{HC}/\omega_{CN} \approx 3/2$. Thus the number of islands in the surfaces of section shown in Fig. 9 reflect the frequency ratios. In a Fourier series expansion of the potential function in action-angle variables, this multiple

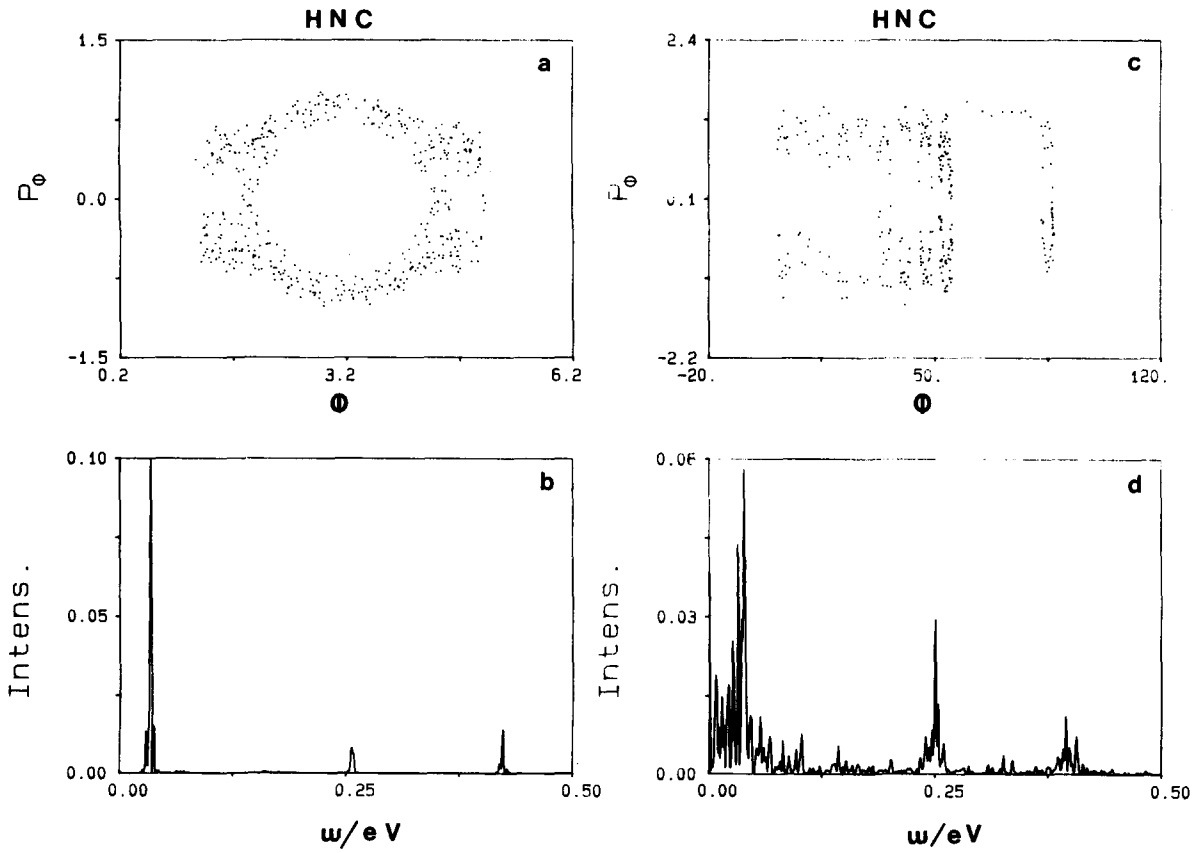

FIG. 7. Chaotic trajectories, (a), (b) localized in the HNC well, $E = 9850\ cm^{-1}$, (c), (d) delocalized at $E = 16\,722\ cm^{-1}$. (a) and (c) are Poincaré surfaces of section in the plane (φ, P_φ) with $R_{HN} = 1.962\ a_0$. (b) and (d) are the power spectra of the sum of the three momenta conjugate to the vibrational coordinates.

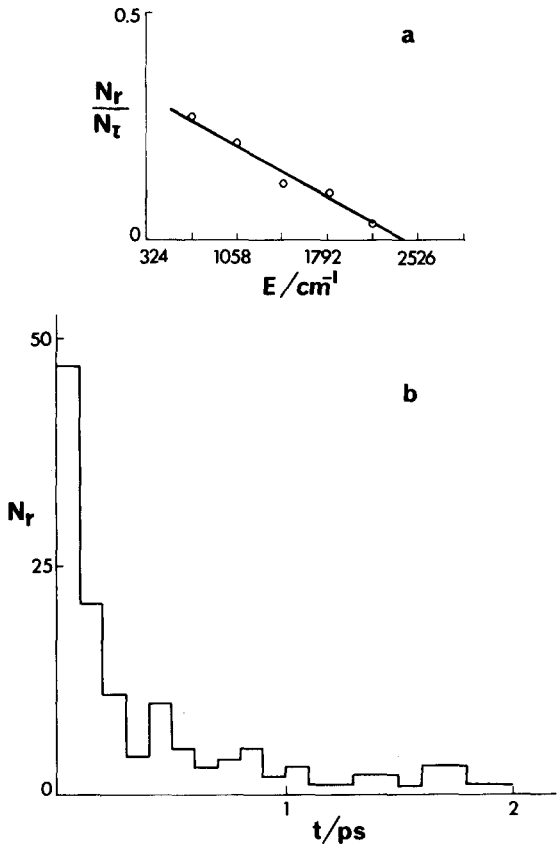

FIG. 8. (a) The proportion of trapped trajectories initialized with zpe in the stretching modes. The abscisa shows the energy in the bending mode above the effective barrier to isomerization (b); the lifetime distribution for the batch of trajectories at $E = 1058$ cm^{-1} above the barrier.

resonance, $\omega_{HC}:\omega_{CN}:\omega_{\varphi} = 6:4:1$, will result in a number of resonant terms,[3] $n_1\omega_{HC} + n_2\omega_{CN} = 0$. For example when n takes the value $(1, 0, -6)$, $(0, 1, -4)$ and linear combinations of them such as $(-1, 1, 2)$ and $(1, 1, -10)$. The smoothness of the curves around the periodic orbit is also the result of the simultaneous validity of Eqs. (2).

It should be emphasized that we have not searched particularly to find resonant trajectories but they come just by randomly sampling the phases of the three oscillators in order to study the isomerization process. Therefore, the fact that such trajectories can be found demonstrates that the multiple resonance influences a considerable part of phase space. Generally the location of multiple periodic orbits in three or even higher dimensional systems is neither easily nor well studied.[34] The scattered points shown in Fig. 9 are from a chaotic trajectory trapped among the islands. The positive Lyapunov exponents shown in Fig. 10 are for one regular and two chaotic trajectories at the same energy as in Fig. 9. For the regular trajectory all Lyapunov exponents tend to zero but for the chaotic trajectories one can see that although the second Lyapunov exponent is small compared to the maximum it has a finite value. This is in accordance with the picture we get from the previous analysis, that is chaos is developed across the reaction coordinate, but it is restricted in the others degrees of freedom.

Excitation of the stretching mode leads to the location of other resonances. Figure 11 shows the $\omega_{HC}:\omega_{CN} = 2:3$ resonance obtained by exciting the CH bond at 13 550 cm^{-1}. Similarly, excitation of the HN bond of HNC reveals the $\omega_{HN}:\omega_{CN} = 2:3$ resonance at the energy 26 170 cm^{-1}. At

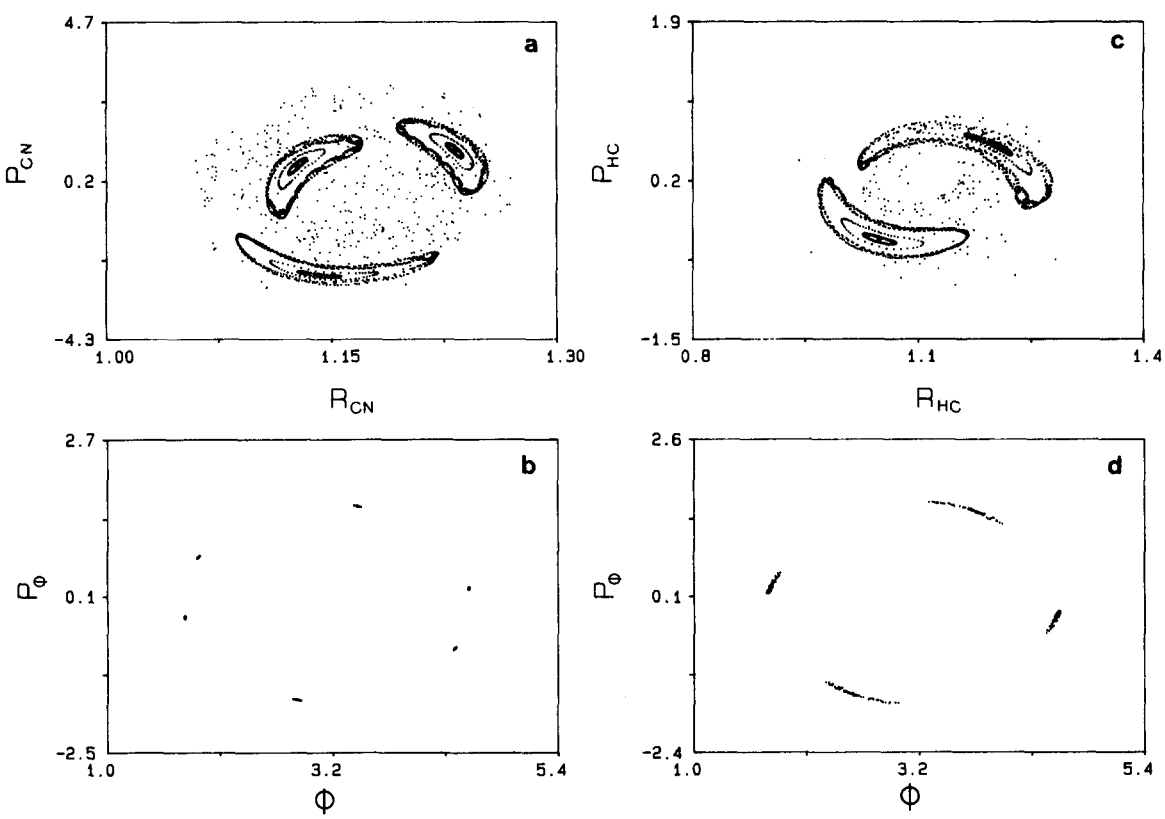

FIG. 9. Poincaré surfaces of sections for the $\omega_{HC}:\omega_{CN}:\omega_{\varphi} = 6:4:1$ resonance at 1058 cm^{-1} above the barrier. In (a) and (c), five trajectories are shown and one of them is chaotic, (b) is the second trajectory from the center of the islands and (d) the outer one.

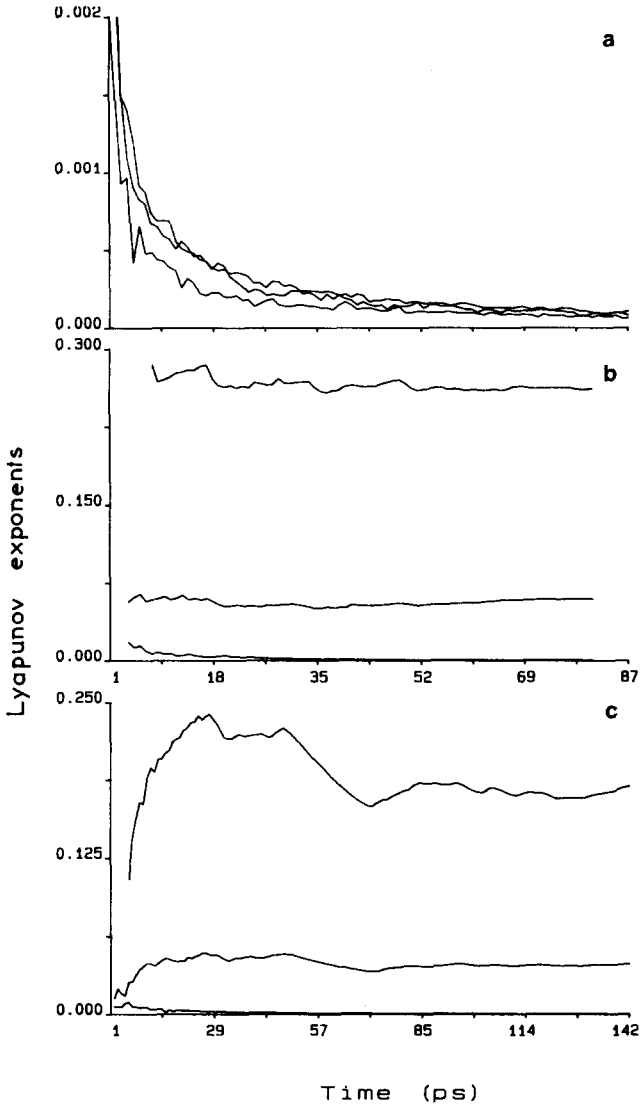

FIG. 10. The positive Lyapunov exponents for trajectories at the same energy as those in Fig. 9(a) is quasiperiodic, (b) and (c) are chaotic.

high excitation energies of CH mode, the 1:1 resonance predominates, whereas stable resonances obtained by exciting the CN bond can be located even above the dissociation threshold, Fig. 12. The existence of isolated resonances up to these energies demonstrate that chaos in the HCN is suppressed.[35]

IV. DISCUSSION

One of the goals of the present work was to compare the regular/chaotic behavior of HCN with respect to KCN and LiCN studied before.[5] It is found both classically and quantum mechanically, that HCN shows an increased regularity compared to LiCN. The conclusion established in the LiCN study, that excitation of the bending mode is the easy route to vibrational chaos, is also confirmed in the present calculations. This route is intimately linked to the presence of a barrier in the potential.

Both the 2D and 3D quantum computations show that extended delocalization of the bending overtones occurs at about 2400 cm^{-1} above the potential barrier to isomerization. Bacic and Light[17] employ the concept of the effective potential, the reaction path in which the two stretching zero-point energies have been added, to explain the delay in delocalization. The 2D results show that the first seriously delocalized state is at about the same energy as in the 3D calculations (the zpe of the 3D calculations is added to the eigenvalues). However, the next state, the 44th (Table I), as well as the 48th and even more at higher energies are of the rotation type which shows that the delocalization is easier in the 2D than in the 3D potential. Notice that the 44th state [Fig. 3(a)] has more amplitude in the HNC minimum than in HCN. Bacic and Light noticed the localization of the wave functions above the effective barrier and comment that this is due to the low bending excitation. However, the two rotating type states (Fig. 3), taking into account that the bending overtones are overestimated in the 2D results, are possibly in the energy range covered in the 3D quantum calculations. As has been shown similar localization of the trajectories is observed in the classical studies. Although it is found that chaotic trajectories can escape from HCN to HNC minimum, when the bending mode is excited just above the barrier, a significant number of them are trapped because of the multiple resonance 6:4:1 among the CH, CN, and φ vibrational modes. This resonance influences the isomerization process up to 2500 cm^{-1} above the effective barrier (Fig. 8).

Could we argue that the classical resonance signals the localization of the eigenfunctions at these energies as well? Strong evidence in favor of the classical–quantum correspondence in a case of a classical resonance comes from a direct comparison of classical, semiclassical, and quantum calculations on a 2D Henon–Heiles model.[36,37] DeLeon *et al.*[37] have demonstrated that the characteristics of a 3:4 resonance are reflected on the nodal structure of the wave functions. Heller[38] has even shown that for the stadium model, the eigenfunctions show an increased density across the unstable periodic orbits. The importance of periodic orbits in a semiclassical quantization has been shown by Gutzwiller[39] and Berry and Tabor.[40] The multiple classical resonance which we have found for HCN is quite broad in energy and phase space and therefore it is expected to mark the quantum behavior of HCN. This is supported by the fact that in the 2D calculations where the motion of CN is suppressed the delocalization of the wave function increases.

The phase space structure for HCN/HNC can be compared with that obtained for a symmetric double well 2D potential of DeLeon and Berne.[41] In this work the isomerization reaction was studied as a function of the coupling between the reaction path and the other coordinate, which was described by a Morse potential. For weak coupling there are crossing and trapping tori. As the coupling increases the crossing tori are destroyed first and then the trapping tori. RRKM-type behavior for isomerization is achieved only after the destruction of all tori. In the realistic case of HCN we also find trapping tori but not crossing ones. This is because chaos starts early in the HNC well in contrast to the HCN. We believe that this is due to the artifact of the potential function inside the HNC minimum.

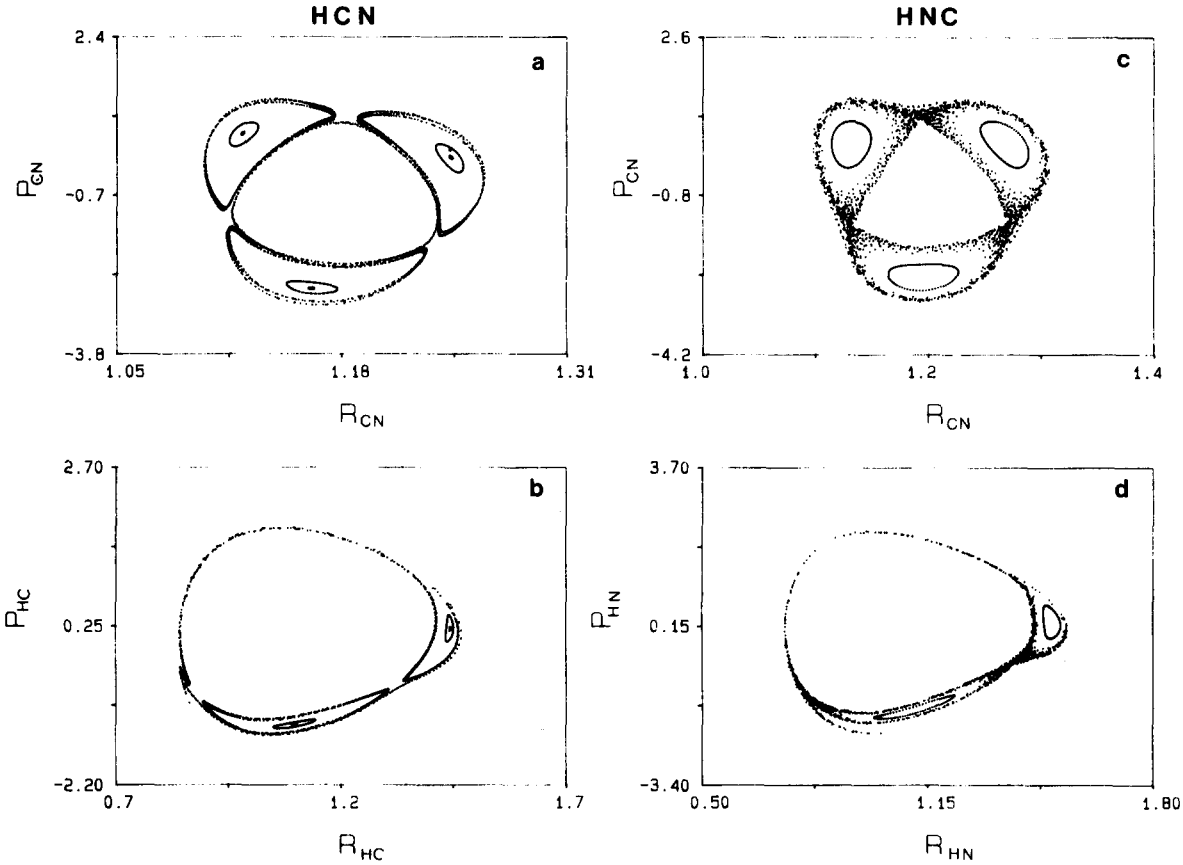

FIG. 11. $\omega_{HC(HN)}:\omega_{CN} = 2:3$ resonances between the stretchig coordinates; (a), (b) for HCN at $E = 13\,541\ cm^{-1}$ and (c), (d) for HNC at $E = 26\,171\ cm^{-1}$.

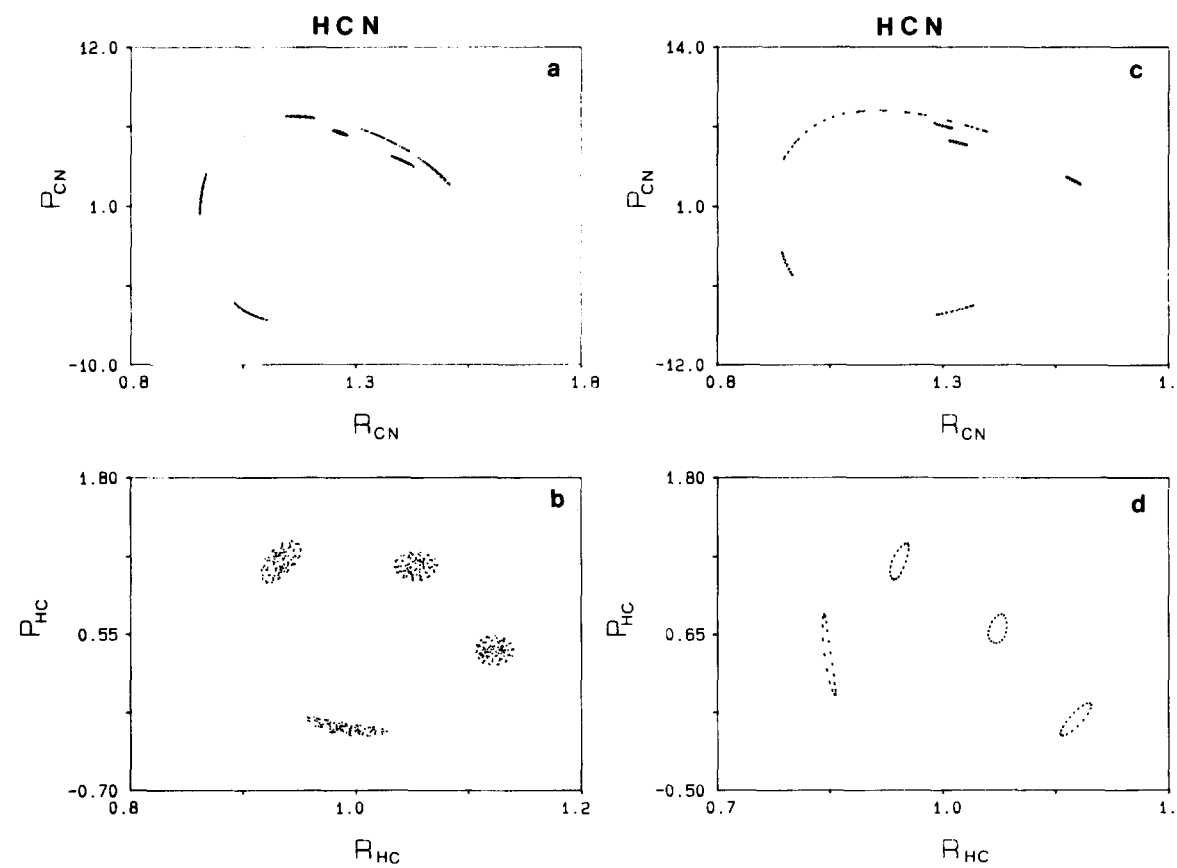

FIG. 12. $\omega_{HC}:\omega_{CN} = 4:6$ resonance (a), (b) for $E = 32\,993\ cm^{-1}$ and (c), (d) for $E = 46\,784\ cm^{-1}$ (above the dissociation threshold).

ACKNOWLEDGMENT

We thank Dr. Bacic and Professor Light for supplying results prior to publication.

[1]D. W. Noid, M. L. Koszykowski, and R. A. Marcus, Annu. Rev. Phys. Chem. **32**, 267 (1981); E. B. Stechel and E. J. Heller, *ibid.* **35**, 563 (1984).
[2]E. Abramson, R. W. Field, D. Imre, K. K. Innes, and J. L. Kinsey, J. Chem. Phys. **83**, 453 (1985); R. L. Sudberg, E. Abramson, J. L. Kinsey, and R. W. Field, *ibid.* **83**, 466 (1985); H. L. Dai, C. L. Korpa, J. L. Kinsey, and R. W. Field, *ibid.* **82**, 1688 (1985); J. L. Hardwick, J. Mol. Spectrosc. **109**, 85 (1985).
[3]A. J. Lichtenderg and M. A. Lieberman, *Regular and Stochastic Motion* (Springer, New York 1983).
[4]R. M. Stratt, N. C. Handy, and W. H. Miller, J. Chem. Phys. **71**, 3311 (1980); E. J. Heller and R. L. Sundberg, in *Chaotic Behavior in Quantum Systems*, edited by G. Casati (Plenum, New York, 1985); S. W. McDonald and A. N. Kaufman, Phys. Rev. Lett. **42**, 1189 (1979).
[5]J. Tennyson and S. C. Farantos, Chem. Phys. Lett. **109** 160 (1984); S. C. Farantos and J. Tennyson, J. Chem. Phys. **82**, 800 (1985).
[6]J. Tennyson and S. C. Farantos, Chem. Phys. **93**, 237 (1985).
[7]S. C. Farantos and J. Tennyson, J. Chem. Phys. **85**, 641 (1986).
[8]J. Tennyson, G. Brocks, and S. C. Farantos, Chem. Phys. **104**, 339 (1986).
[9]J. Tennyson, Mol. Phys. **55**, 463 (1985).
[10]S. C. Farantos and J. Tennyson, in *Stochasticity and Intramolecular Redistribution of Energy*, edited by R. Lefevbre and S. Mukamel (Reidel, Orsay, 1987).
[11]M. V. Berry and M. Tabor, Proc. R. Soc. London Ser. A **356**, 375 (1977).
[12]O. Bohigas, M. J. Giannoni, and C. Schmit, Phys. Rev. Lett. **52**, 1 (1984).
[13]I. C. Percival, Adv. Chem. Phys. **36**, 1 (1977).
[14]G. Brocks, Chem. Phys. **116**, 33 (1987).
[15]G. S. Ezra, Chem. Phys. Lett. **127**, 492 (1986).
[16]S. C. Farantos and N. Flytzanis, J. Chem. Phys. **87**, 6449 (1987).
[17]Z. Bacic and J. C. Light, J. Chem. Phys. **86**, 3065 (1987).
[18]M. Peric, M. Mladenovic, S. D. Peyerimhoff, and R. J. Buenker, Chem. Phys. **82**, 317 (1983); **86**, 85 (1984).
[19]Z. Bacic, R. B. Gerber, and M. A. Ratner, J. Phys. Chem. **90**, 3606 (1986).
[20]J. N. Murrell, S. Carter, and L. O. Halonen, J. Mol. Spectrosc. **93**, 307 (1982).
[21]T. A. Holme and J. S. Hutchinson, J. Chem. Phys. **83**, 2860 (1985).
[22]K. K. Lehmann, G. J. Scherer, and W. Klemperer, J. Chem. Phys. **77**, 2853 (1982); **78**, 608 (1983).
[23]A. Wolf, J. B. Swiff, H. Z. Swinney, and J. A. Vartano, Physica D **16**, 285 (1985).
[24]G. Benettin, L. Galgani, and J. M. Strelcyn, Phys. Rev. A**14**, 2338 (1976).
[25]H. D. Meyer, J. Chem. Phys. **84**, 3147 (1986).
[26]G. Contopoulos, L. Galgani, and A. Giorgilli Phys. Rev. A **18**, 1183 (1978).
[27]N. N. Nekhoroshev, Usp. Mat. Nauk. **32**, 5 (1977) [English translation, Russ. Math. Surv. **32**, 1, (1977)]; G. Bennetin, L. Galgani, and A. Giorgilli, Nuovo Cimento, B **89**, 103 (1985).
[28]W. P. Reinhardt, in *The Mathematical Analysis of Physical Systems*, edited by R. Mickens (Van Nostrand, New York, 1984).
[29]D. W. Noid, M. L. Koszykowski, and R. A. Marcus, J. Chem. Phys. **73**, 391 (1980).
[30]M. Henon, Physica D **5**, 412 (1985).
[31]B. T. Sutcliffe and J. Tennyson, Mol. Phys. **58**, 1053 (1986).
[32]B. T. Sutcliffe and J. Tennyson, in *Molecules in Physics, Chemistry and Biology*, eidted by I. Csizmadia and J. Maruami (Reidel, Dordrecht, 1987).
[33]J. Tennyson, Comput. Phys. Commun. **42**, 257 (1986); Comput. Phys. Rep. **4**, 1 (1986).
[34]M. Founargiotakis and S. C. Farantos (work in progress).
[35]B. V. Chirikov, Phys. Rep. **52**, 263 (1979).
[36]E. J. Heller, E. B. Stechel, and M. J. Davis, J. Chem. Phys. **73**, 4720 (1980).
[37]N. DeLeon, M. J. Davis, and E. J. Heller, J. Chem. Phys. **80**, 794 (1984).
[38]E. J. Heller, Phys. Rev. Lett. **53**, 1515 (1984).
[39]M. C. Gutzwiller, Physica D **5**, 183 (1982).
[40]M. V. Berry and N. Tabor, Proc. R. Soc. London Ser. A **349**, 101 (1976).
[41]N. DeLeon and B. J. Berne, J. Chem. Phys. **75**, 3495 (1981).